

Crucially, this expansion work depends on both the initial size of the transient voids and on any intra- or intermolecular interactions that oppose expansion.^{25–28} This framework for gas absorption in liquids provides two routes to increase absorption capacity: (1) manipulating the free volume to increase the size and/or frequency of transient voids and (2) reducing the magnitude of expansion work. Both of these factors are thought to contribute to the high gas solubilities of perfluorocarbon solvents, which have the highest O₂ solubilities of any liquid under ambient conditions³⁰ and have received significant attention as O₂ carriers for biomedical applications.³¹

Though free volume has been recognized to play an important role in the gas absorption properties of ionic liquids,^{12,32,33} direct experimental probes of free volume have been limited. Moreover, long-standing and fundamental inconsistencies in how free volume is defined and measured³⁴—including both total free volume and the size distribution of transient voids—have made it difficult to rationalize gas solubility trends in ionic liquids. For instance, refractive index measurements have suggested that ionic liquids contain up to 75% free volume,³⁵ while group contribution methods have been used to estimate free volume fractions in the range of 10–25%.¹² In addition, molar volume has frequently been used as a qualitative proxy for fractional free volume within a series of similar ionic liquids, even though molar volume generally does not correlate with volumetric gas absorption capacity in these systems.^{17,33,36–38} Similar to the total free volume, reported void sizes for ionic liquids have ranged from average diameters of 6–10 Å based on positron annihilation lifetime spectroscopy^{9,13,14,39,40} and ¹²⁹Xe NMR^{14,41} measurements to less than 4 Å based on molecular dynamics (MD) simulations,^{42–46} even for the same ionic liquid.

Here, we report a new approach to evaluate free volume in ionic liquids through the measurement of isothermal compressibility by small-angle X-ray scattering (SAXS). Specifically, we use a combination of gas absorption measurements, SAXS, variable temperature densimetry, and MD simulations to understand trends in O₂ absorption capacities for a diverse series of ionic liquids that includes imidazolium and phosphonium cations and fluorinated anions and cations. Our results reveal the important role that void size distributions play in determining the amount of O₂ that is absorbed in an ionic liquid and provide design strategies for targeting ionic liquids with higher gas capacities.

RESULTS AND DISCUSSION

O₂ Absorption Isotherms. Gas absorption isotherms are integral to establish relationships between the composition of an ionic liquid and its ability to dissolve and transport gas molecules. Performing accurate O₂ absorption measurements in ionic liquids near ambient pressure and temperature, however, is challenging due to both the low amount of gas that is absorbed—particularly in comparison to microporous solids—and the slow absorption kinetics that can result from high liquid viscosities. Indeed, there are large discrepancies in the reported O₂ absorption capacities even among the relatively small number of ionic liquids for which O₂ absorption has been quantified (Table S2).³⁰

After careful calibration and validation of a volumetric absorption instrument (see the Supporting Information), we measured O₂ absorption isotherms at 25 °C from 0.2 to 1 bar

for a representative set of eight ionic liquids encompassing a diversity of cations and anions (Figure 1). Though

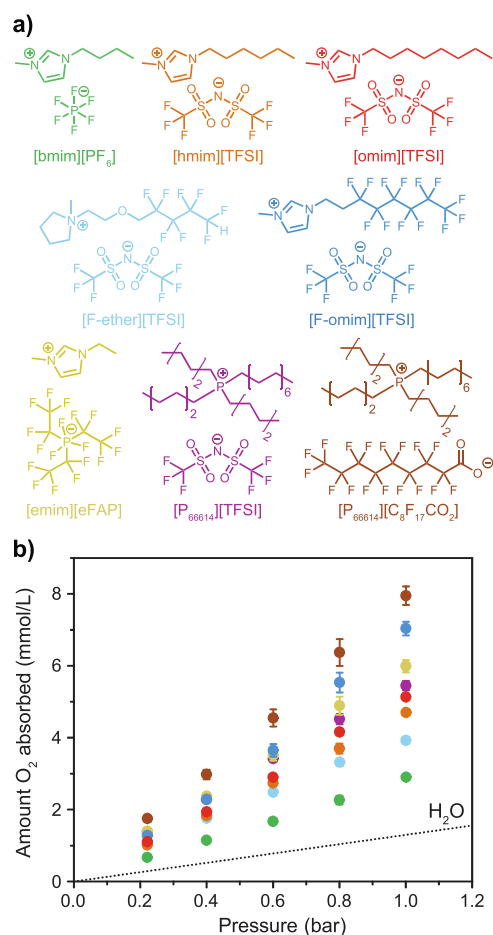


Figure 1. (a) Chemical structures and abbreviations for the series of ionic liquids studied in this work. (b) Amount of O₂ absorbed in terms of mmol O₂ per L of ionic liquid as a function of pressure at 25 °C. As a reference, the O₂ solubility of H₂O is shown as a dotted black line. Brown, dark blue, yellow, purple, red, orange, light blue, and green dots represent the absorption isotherm data for [P₆₆₆₁₄]-[C₈F₁₇CO₂], [F-omim][TFSI], [emim][eFAP], [P₆₆₆₁₄][TFSI], [omim][TFSI], [hmim][TFSI], [F-ether][TFSI], and [bmim][PF₆], respectively. Error bars represent the standard deviation calculated based on blank measurements (Figure S23). Note that the error bars are smaller than the size of the data point in some cases.

perfluorocarbon solvents exhibit some of the highest solubilities for nonpolar gases under ambient conditions, the O₂ absorption properties of fluorinated ionic liquids have received only limited attention.^{47,48} As such, our library of ionic liquids includes two perfluorinated anions and two cations with partially fluorinated alkyl chains. In particular, we chose to examine the ionic liquid [F-ether][TFSI], which is composed of a TFSI anion [TFSI = bis(trifluoromethane)-sulfonimide] and a pyrrolidinium cation with a partially fluorinated ether chain because previous electrochemical measurements suggested that this ionic liquid has an O₂ absorption capacity of 34 mmol/L at 25 °C and 1 bar,⁴⁸ which would be comparable to perfluorocarbon solvents and would far exceed the absorption capacities reported for any other ionic liquid.³⁰

As expected, all O₂ adsorption isotherms are in the Henry's law regime—linear with respect to pressure. Moreover, the two ionic liquids with the most heavily fluorinated alkyl chains exhibit the highest O₂ absorption capacities. Specifically, [F-omim][TFSI] has the second-highest O₂ absorption capacity (7.0 mmol/L at 1 bar) of the ionic liquids measured in this work, which is 37% higher than its hydrocarbon analogue [omim][TFSI]. In addition, the ionic liquid [P₆₆₆₁₄]-[C₈F₁₇CO₂], which contains an alkylphosphonium cation and a perfluorinated alkylcarboxylate anion, has the highest O₂ absorption capacity of 8.0 mmol/L at 1 bar. This O₂ capacity is 45% higher than that of [P₆₆₆₁₄][TFSI], which contains the same alkylphosphonium cation and a TFSI anion, emphasizing the role of the perfluorinated alkyl chain in promoting O₂ absorption.

The high O₂ capacities observed for [F-omim][TFSI] and [P₆₆₆₁₄][C₈F₁₇CO₂] cannot be attributed to specific interactions between O₂ and C–F bonds, as these types of interactions do not occur in neutral perfluorocarbon solvents.⁴⁹ Interestingly, [F-ether][TFSI] has an O₂ absorption capacity of only 3.9 mmol/L, which is nearly an order of magnitude lower than the previously reported value of 34 mmol/L.⁴⁸ This difference may be due to uncertainties associated with extrapolating gas solubilities from electrochemical experiments and emphasizes the importance of direct gas absorption measurements. Still, the lower O₂ absorption capacity of [F-ether][TFSI] compared to [hmim][TFSI] and [omim][TFSI]—both of which have hydrocarbon-based cations—is somewhat surprising and may be related to differences in intra- or intermolecular interactions that result from the presence of an ether linkage or pyrrolidinium cation.

To better understand these trends, we explored experimental probes of ionic liquid structure and free volume that could provide insights into the factors that influence O₂ absorption. Despite the many previous examples where molar volume has been used as a qualitative proxy for free volume, we observe a poor correlation ($r^2 = 0.52$) between molar volume and gas capacity (Figure S26). Indeed, [F-ether][TFSI] and [F-omim][TFSI] have very similar molar volumes, but the latter absorbs 80% more O₂. This observation highlights that there is no physical basis for why molar volume should directly correlate with gas absorption capacities across different ionic liquids. High molar volumes may sometimes be correlated with bulkier or stiffer molecules that form liquids with increased free volume and higher gas solubilities, but there is no fundamental reason why molecular size should have a strong correlation with gas solubility, particularly across a diverse range of ionic liquids. As such, more direct and universal descriptors of ionic liquid structure are needed to explain trends in gas absorption.

Isothermal Compressibility. The higher O₂ solubility of perfluorocarbon solvents compared to hydrocarbon solvents has been attributed to the presence of more free volume and larger transient voids, which is reflected by the higher isothermal compressibilities of perfluorocarbons.^{50,51} With this in mind, we hypothesized that isothermal compressibility might similarly provide a useful probe of free volume in ionic liquids and could lend insights into trends in absorption behavior. In particular, the isothermal compressibility of a liquid can be determined from SAXS experiments, which are easier to perform on small amounts of sample than more traditional mechanical measurements.⁵² Though SAXS has been widely used to measure the isothermal compressibility of water in different environments,⁵³ it has, to the best of our

knowledge, yet to be applied to measure the isothermal compressibility of an ionic liquid.

The free volume present within a liquid is directly responsible for the connection between SAXS and isothermal compressibility. As previously mentioned, dynamic free volume emerges from molecular-level fluctuations in density that create—and destroy—transient voids. Conceptually, larger transient voids and more free volume will coincide with greater density fluctuations within a liquid. Mathematically, the magnitude of X-ray scattering intensity, $S(q)$, at zero scattering angle, $q \rightarrow 0$, is related to the magnitude of local fluctuations in number density, N , from the average number density of the bulk liquid, $\langle N \rangle$, as expressed by⁵³

$$\lim_{q \rightarrow 0} S(q) = \frac{\langle (N - \langle N \rangle)^2 \rangle}{\langle N \rangle} \quad (1)$$

Using statistical mechanics, these density fluctuations can be directly related to isothermal compressibility, β_T , by

$$\frac{\langle (N - \langle N \rangle)^2 \rangle}{\langle N \rangle} = \frac{\beta_T k_B T}{v} \quad (2)$$

where k_B is the Boltzmann constant, T is the temperature, and v is the mean volume per molecule.⁵⁴

After confirming that the isothermal compressibilities calculated from SAXS data for *n*-hexane and three perfluorocarbon liquids were in close agreement with literature values determined by other techniques (Table S1), we performed SAXS experiments to measure the isothermal compressibility of each of the ionic liquids evaluated for O₂ absorption. To accurately determine the isothermal compressibility of an ionic liquid from SAXS data, it is critical to select a region of q for which X-ray scattering results entirely from density fluctuations and does not have any structural contributions. Except for the ionic liquid [P₆₆₆₁₄][C₈F₁₇CO₂], such a region (generally from 0.05 to 0.1 Å⁻¹) was present in the scattering data for each ionic liquid, allowing isothermal compressibilities to be extracted (Figure 2).

As anticipated, we observe a strong correlation between isothermal compressibility and the amount of O₂ absorbed at 1

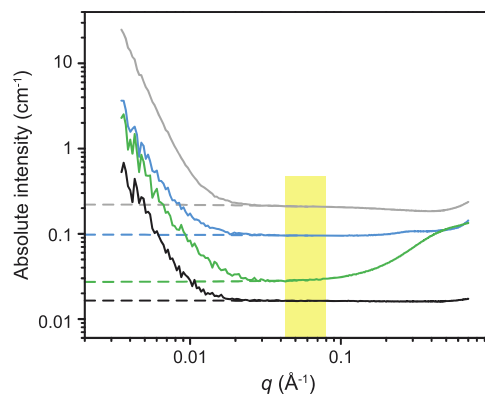


Figure 2. Absolute SAXS intensity as a function of scattering angle, q , for perfluorohexane (C₆F₁₄, gray), [F-omim][TFSI] (blue), [bmim][PF₆] (green), and H₂O (black). Absolute intensities were calculated from raw arbitrary intensities by calibrating to the compressibility of H₂O as a standard. Dashed lines represent linear extrapolations to $q \rightarrow 0$ from the region of q highlighted in yellow. Note that a featureless region such as the one highlighted in yellow is required to accurately extrapolate absolute SAXS intensities to $q \rightarrow 0$.

bar and 25 °C (Figure 3a), with ionic liquids with low O₂ capacities, such as [bmim][PF₆] and [F-ether][TFSI], having

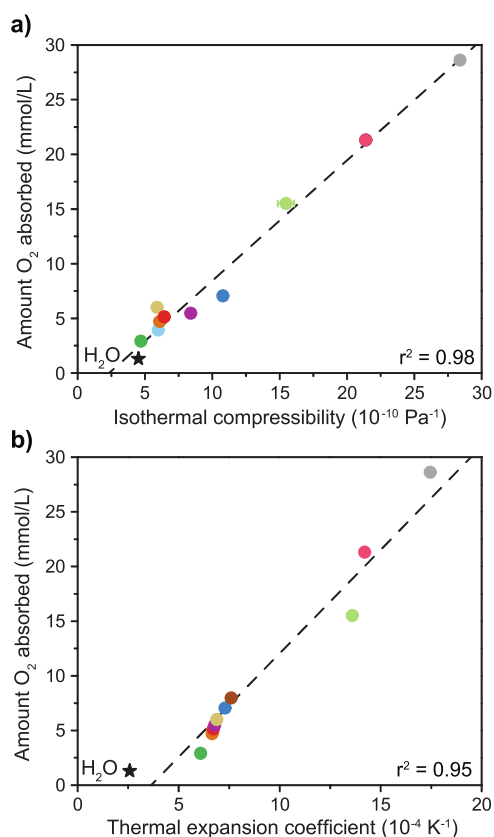


Figure 3. (a) Amount of O₂ absorbed in mmol O₂ per L of liquid at 25 °C and 1 bar as a function of isothermal compressibility at 25 °C and ambient pressure. (b) Amount of O₂ absorbed in mmol O₂ per L of liquid at 25 °C and 1 bar as a function of thermal expansion coefficient at 25 °C and ambient pressure. Neutral solvents, including perfluorohexane (C₆F₁₄, gray), perfluoromethylcyclohexane (pink), and hexane (C₆H₁₄, light green), are compared to the ionic liquids [P₆₆₆₁₄][C₈F₁₇CO₂] (brown), [F-omim][TFSI] (dark blue), [emim][eFAP] (yellow), [P₆₆₆₁₄][TFSI] (purple), [omim][TFSI] (red), [hmim][TFSI] (orange), [F-ether][TFSI] (light blue), and [bmim][PF₆] (green). The dashed line represents a linear fit to the data. Note that accurate isothermal compressibility data could not be obtained for [P₆₆₆₁₄][C₈F₁₇CO₂] due to interference from the intermolecular structure in the SAXS pattern (Figure S24).

much lower compressibilities than those with high O₂ capacities, such as [F-omim][TFSI]. The higher isothermal compressibility of [F-omim][TFSI] is consistent with the increased rigidity and weaker intermolecular interactions characteristic of perfluorocarbons.⁵⁵ These weak interactions are also reflected in the higher thermal expansion coefficients of more heavily fluorinated ionic liquids (Figure 3b). Thermal expansion coefficients, which have been qualitatively linked to free volume and CO₂ absorption in ionic liquids previously,⁵⁶ do not exhibit as much variation across the ionic liquids studied here as does isothermal compressibility, but both properties are strongly correlated with O₂ solubility.

The correlation between isothermal compressibility and O₂ absorption provides a direct experimental confirmation of the importance of free volume in designing ionic liquids with high O₂ solubilities. Intriguingly, the relationship between isothermal compressibility and O₂ absorption extends beyond this

set of ionic liquids to molecular liquids with much higher O₂ solubilities, including *n*-hexane and several perfluorocarbons. This suggests that more compressible ionic liquids—perhaps achieved through combinations of anions and cations that both feature perfluorinated alkyl chains—could feature even higher O₂ absorption capacities.

MD Simulations. To better understand relationships between isothermal compressibility, free volume, and O₂ solubility at a molecular level, we performed MD simulations of three representative ionic liquids: (1) the canonical ionic liquid [bmim][PF₆], which has the lowest O₂ solubility measured in this work, (2) [F-omim][TFSI], which has an imidazolium cation with a highly fluorinated alkyl chain [(CH₂)₂(CF₂)₅CF₃] and an O₂ solubility that is 2.4 times higher than [bmim][PF₆], and (3) its hydrocarbon analogue [omim][TFSI]. We utilized an open-source force field that has been previously used to reliably capture the structure and interactions in fluorinated and hydrocarbon ionic liquids (full details in the Supporting Information).⁵⁷ This force field contains parameters tailored specifically for the anions and cations considered in this work rather than relying on generic force field parameters, which is of particular importance given the complex interactions arising from perfluorinated alkyl chains. To validate the force fields used in the simulations, we verified that the simulated densities between 300 and 360 K at ambient pressure matched experimental densities (Figure S25a). We then calculated the isothermal compressibility of each ionic liquid and confirmed that the simulation reproduced the experimentally observed trend in compressibility with [bmim][PF₆] < [omim][TFSI] < [F-omim][TFSI]. The agreement between simulated and experimental compressibilities confirms the reliability of the simulated liquid structure (Figure S25b).

We used stochastic insertions of spherical probes to calculate void size distributions and fractional free volumes for each ionic liquid (Figure 4). Here, the void size distributions represent the probability of a randomly chosen void having a given volume. Though [omim][TFSI] has a 30% higher compressibility and a 50% higher O₂ absorption capacity than

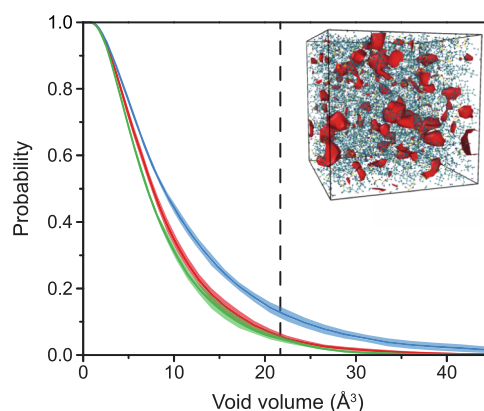


Figure 4. Probability that a randomly chosen void has a particular volume for the ionic liquids [F-omim][TFSI] (blue), [omim][TFSI] (red), and [bmim][PF₆] (green). The shaded area represents the standard deviation of multiple snapshots from five simulation runs beginning from different conditions. The dashed line indicates the volume of an O₂ molecule, assuming a sphere with a kinetic diameter of 3.46 Å.²⁹ Inset: representative snapshot of the voids (red) in [F-omim][TFSI] from MD simulations.

[bmim][PF₆], the two ionic liquids have relatively similar void size distributions and free volumes, with [bmim][PF₆] containing a slightly lower frequency of larger voids and a slightly smaller fractional free volume (0.093 ± 0.002 vs 0.087 ± 0.002). These small differences in void size distributions and free volume may contribute to the difference in O₂ solubility, but other factors that impact the ease with which empty space can be created within the ionic liquid—such as anion rigidity or conformational flexibility of alkyl chains of varying lengths on the imidazolium cations—also likely play an important role.

Notably, the void size distribution for [F-omim][TFSI]—the ionic liquid with the highest isothermal compressibility—is more broad than those for the other two ionic liquids, indicating that larger voids form at a higher frequency than in the less compressible ionic liquids. This general trend is consistent with previous simulations of [F-omim][TFSI] and [omim][TFSI], which were performed with slightly different parameters and suggested a much more subtle difference in void size distributions than observed here.⁵⁸ Interestingly, our simulations also reveal that the fractional free volume of [F-omim][TFSI] (0.090 ± 0.002) is within error of that of [omim][TFSI] (0.093 ± 0.002). This result implies that [F-omim][TFSI] has a smaller total number of voids than the nonfluorinated ionic liquids, but that on average, each void is larger. This larger void size in [F-omim][TFSI] compared to [omim][TFSI] may be due to the higher rigidity and poor interaction geometry of fluorinated chains, an effect that has been previously observed for neutral perfluorocarbon liquids.⁵⁵ As such, the presence of a greater density of larger voids—rather than any difference in total free volume—likely contributes to the higher O₂ solubility of the fluorinated ionic liquid, wherein there is a greater probability of a void forming that is large enough to accommodate an O₂ molecule than in the nonfluorinated ionic liquid.

CONCLUSIONS

These results show that isothermal compressibility measurements via SAXS are a powerful tool for probing free volume in ionic liquids and understanding trends in gas absorption. In particular, we show that fluorinated ionic liquids feature large isothermal compressibilities and increased O₂ absorption capacities, which result, at a microscopic level, from a higher frequency of large transient voids. Efforts to develop more highly fluorinated ionic liquids capable of absorbing even greater capacities of nonpolar gases and to evaluate isothermal compressibilities and void size distributions across a wider range of ionic liquids are currently in progress.

ASSOCIATED CONTENT

Supporting Information

The Supporting Information is available free of charge at <https://pubs.acs.org/doi/10.1021/acs.jpcb.2c00202>.

Additional experimental details, NMR data, SAXS analysis, and simulation details (PDF)

AUTHOR INFORMATION

Corresponding Authors

Boris Kozinsky – John A. Paulson School of Engineering and Applied Sciences, Harvard University, Cambridge, Massachusetts 02138, United States; orcid.org/0000-0002-0638-539X; Email: bkoz@seas.harvard.edu

Jarad A. Mason – Department of Chemistry and Chemical Biology, Harvard University, Cambridge, Massachusetts 02138, United States; orcid.org/0000-0003-0328-7775; Email: mason@chemistry.harvard.edu

Authors

Malia B. Wenny – Department of Chemistry and Chemical Biology, Harvard University, Cambridge, Massachusetts 02138, United States

Nicola Molinari – John A. Paulson School of Engineering and Applied Sciences, Harvard University, Cambridge, Massachusetts 02138, United States; orcid.org/0000-0002-2913-7030

Adam H. Slavney – Department of Chemistry and Chemical Biology, Harvard University, Cambridge, Massachusetts 02138, United States

Surendra Thapa – Department of Chemistry and Chemical Biology, Harvard University, Cambridge, Massachusetts 02138, United States

Byeongdu Lee – Advanced Photon Source, Argonne National Laboratory, Argonne, Illinois 60439, United States; orcid.org/0000-0003-2514-8805

Complete contact information is available at: <https://pubs.acs.org/10.1021/acs.jpcb.2c00202>

Notes

The authors declare no competing financial interest.

ACKNOWLEDGMENTS

This work used beamline 12-ID-B at the Advanced Photon Source, a U.S. Department of Energy (DOE) Office of Science User Facility operated for the DOE Office of Science by Argonne National Laboratory under contract no. DE-AC02-06CH11357. This research was supported under a Multidisciplinary University Research Initiative, sponsored by the Department of the Navy, Office of Naval Research, under grant N00014-20-1-2418. M.B.W. is supported by the Department of Energy Computational Science Graduate Fellowship under grant DE-FG02-97ER25308. J.A.M. acknowledges support from the Arnold and Mabel Beckman Foundation through a Beckman Young Investigator grant.

REFERENCES

- (1) Eyring, H.; Hirschfelder, J. The Theory of the Liquid State. *J. Phys. Chem.* **1937**, *41*, 249–257.
- (2) Lennard-Jones, J. E.; Evonshire, A. F. D. Critical Phenomena in Gases—I. *Proc. R. Soc. London, Ser. A* **1937**, *163*, 53–70.
- (3) Bondi, A. Free Volumes and Free Rotation in Simple Liquids and Liquid Saturated Hydrocarbons. *J. Phys. Chem.* **1954**, *58*, 929–939.
- (4) Sastry, S.; Truskett, T. M.; Debenedetti, P. G.; Torquato, S.; Stillinger, F. H. Free Volume in the Hard Sphere Liquid. *Mol. Phys.* **1998**, *95*, 289–297.
- (5) Doolittle, A. K. Studies in Newtonian Flow. II. the Dependence of the Viscosity of Liquids on Free-Space. *J. Appl. Phys.* **1951**, *22*, 1471–1475.
- (6) Cohen, M. H.; Turnbull, D. Molecular Transport in Liquids and Glasses. *J. Chem. Phys.* **1959**, *31*, 1164–1169.
- (7) Miller, A. A. Free Volume and Viscosity of Liquids: Effects of Temperature. *J. Phys. Chem.* **1963**, *67*, 1031–1035.
- (8) Miyamoto, T.; Shibayama, K. Free-volume Model for Ionic Conductivity in Polymers. *J. Appl. Phys.* **1973**, *44*, 5372–5376.
- (9) Beichel, W.; Yu, Y.; Dlubek, G.; Krause-Rehberg, R.; Pionteck, J.; Pfefferkorn, D.; Bulut, S.; Bejan, D.; Friedrich, C.; Krossing, I. Free Volume in Ionic Liquids: A Connection of Experimentally Accessible

- Observables from PALS and PVT Experiments with the Molecular Structure from XRD Data. *Phys. Chem. Chem. Phys.* **2013**, *15*, 8821.
- (10) Eley, D. D. On the Solubility of Gases. Part I.—The Inert Gases in Water. *Trans. Faraday Soc.* **1939**, *35*, 1281–1293.
- (11) Fürth, R.; Born, M. On the Theory of the Liquid State: I. The Statistical Treatment of the Thermodynamics of Liquids by the Theory of Holes. *Math. Proc. Cambridge Philos. Soc.* **1941**, *37*, 252–275.
- (12) Shannon, M. S.; Tedstone, J. M.; Danielsen, S. P. O.; Hindman, M. S.; Irvin, A. C.; Bara, J. E. Free Volume as the Basis of Gas Solubility and Selectivity in Imidazolium-Based Ionic Liquids. *Ind. Eng. Chem. Res.* **2012**, *51*, 5565–5576.
- (13) Yu, Y.; Beichel, W.; Dlubek, G.; Krause-Rehberg, R.; Paluch, M.; Pionteck, J.; Pfefferkorn, D.; Bulut, S.; Friedrich, C.; Pogodina, N.; et al. Free Volume and Phase Transitions of 1-Butyl-3-Methylimidazolium Based Ionic Liquids from Positron Lifetime Spectroscopy. *Phys. Chem. Chem. Phys.* **2012**, *14*, 6856.
- (14) Brooks, N. J.; Castiglione, F.; Doherty, C. M.; Dolan, A.; Hill, A. J.; Hunt, P. A.; Matthews, R. P.; Mauri, M.; Mele, A.; Simonutti, R.; et al. Linking the Structures, Free Volumes, and Properties of Ionic Liquid Mixtures. *Chem. Sci.* **2017**, *8*, 6359–6374.
- (15) Welton, T. Ionic Liquids: A Brief History. *Biophys. Rev.* **2018**, *10*, 691–706.
- (16) Carvalho, P. J.; Kurnia, K. A.; Coutinho, J. A. P. Dispelling Some Myths about the CO₂ Solubility in Ionic Liquids. *Phys. Chem. Chem. Phys.* **2016**, *18*, 14757–14771.
- (17) Aki, S. N. V. K.; Mellein, B. R.; Saurer, E. M.; Brennecke, J. F. High-Pressure Phase Behavior of Carbon Dioxide with Imidazolium-Based Ionic Liquids. *J. Phys. Chem. B* **2004**, *108*, 20355–20365.
- (18) Lei, Z.; Dai, C.; Chen, B. Gas Solubility in Ionic Liquids. *Chem. Rev.* **2014**, *114*, 1289–1326.
- (19) Farris, A. L.; Rindone, A. N.; Grayson, W. L. Oxygen Delivering Biomaterials for Tissue Engineering. *J. Mater. Chem. B* **2016**, *4*, 3422–3432.
- (20) Snyder, J.; Fujita, T.; Chen, M. W.; Erlebacher, J. Oxygen Reduction in Nanoporous Metal-Ionic Liquid Composite Electrocatalysts. *Nat. Mater.* **2010**, *9*, 904–907.
- (21) Rodrigues, R. M.; Guan, X.; Iñiguez, J. A.; Estabrook, D. A.; Chapman, J. O.; Huang, S.; Sletten, E. M.; Liu, C. Perfluorocarbon Nanoemulsion Promotes the Delivery of Reducing Equivalents for Electricity-Driven Microbial CO₂ Reduction. *Nat. Catal.* **2019**, *2*, 407–414.
- (22) Kang, C. S. M.; Zhang, X.; Macfarlane, D. R. Synthesis and Physicochemical Properties of Fluorinated Ionic Liquids with High Nitrogen Gas Solubility. *J. Phys. Chem. C* **2018**, *122*, 24550–24558.
- (23) Scherer, G. Interfacial Aspects in the Development of Polymer Electrolyte Fuel Cells. *Solid State Ionics* **1997**, *94*, 249–257.
- (24) Christensen, J.; Albertus, P.; Sanchez-Carrera, R. S.; Lohmann, T.; Kozinsky, B.; Liedtke, R.; Ahmed, J.; Kojic, A. A Critical Review of Li/Air Batteries. *J. Electrochem. Soc.* **2011**, *159*, R1–R30.
- (25) Reiss, H.; Frisch, H. L.; Lebowitz, J. L. Statistical Mechanics of Rigid Spheres. *J. Chem. Phys.* **1959**, *31*, 369–380.
- (26) Pierotti, R. A. The Solubility of Gases in Liquids. *J. Phys. Chem.* **1963**, *67*, 1840–1845.
- (27) Pollack, G. L. Why Gases Dissolve in Liquids. *Science* **1991**, *251*, 1323–1330.
- (28) Hu, Y.-F.; Liu, Z.-C.; Xu, C.-M.; Zhang, X.-M. The Molecular Characteristics Dominating the Solubility of Gases in Ionic Liquids. *Chem. Soc. Rev.* **2011**, *40*, 3802–3823.
- (29) Mehio, N.; Dai, S.; Jiang, D.-e. Quantum Mechanical Basis for Kinetic Diameters of Small Gaseous Molecules. *J. Phys. Chem. A* **2014**, *118*, 1150–1154.
- (30) Miyamoto, H.; Yampolski, Y.; Young, C. L. IUPAC-NIST Solubility Data Series. 103. Oxygen and Ozone in Water, Aqueous Solutions, and Organic Liquids (Supplement to Solubility Data Series Volume 7). *J. Phys. Chem. Ref. Data* **2014**, *43*, 033102.
- (31) Riess, J. G. Oxygen Carriers (“Blood Substitutes”)—Raison d’être, Chemistry, and Some Physiology. *Chem. Rev.* **2001**, *101*, 2797–2920.
- (32) Kazarian, S. G.; Briscoe, B. J.; Welton, T. Combining Ionic Liquids and Supercritical Fluids: In Situ ATR-IR Study of CO₂ Dissolved in Two Ionic Liquids at High Pressures. *Chem. Commun.* **2000**, 2047–2048.
- (33) Blanchard, L. A.; Gu, Z.; Brennecke, J. F. High-Pressure Phase Behavior of Ionic Liquid/CO₂ Systems. *J. Phys. Chem. B* **2001**, *105*, 2437–2444.
- (34) Bondi, A. Free Volumes and Free Rotation in Simple Liquids and Liquid Saturated Hydrocarbons. *J. Phys. Chem.* **1954**, *58*, 929–939.
- (35) Pereira, A. B.; Araújo, J. M. M.; Martinho, S.; Alves, F.; Nunes, S.; Matias, A.; Duarte, C. M. M.; Rebelo, L. P. N.; Marrucho, I. M. Fluorinated Ionic Liquids: Properties and Applications. *ACS Sustainable Chem. Eng.* **2013**, *1*, 427–439.
- (36) Muldoon, M. J.; Aki, S. N. V. K.; Anderson, J. L.; Dixon, J. K.; Brennecke, J. F. Improving Carbon Dioxide Solubility in Ionic Liquids. *J. Phys. Chem. B* **2007**, *111*, 9001–9009.
- (37) Palgunadi, J.; Kang, J. E.; Nguyen, D. Q.; Kim, J. H.; Min, B. K.; Lee, S. D.; Kim, H.; Kim, H. S. Solubility of CO₂ in Dialkylimidazolium Dialkylphosphate Ionic Liquids. *Thermochim. Acta* **2009**, *494*, 94–98.
- (38) Zhang, X.; Huo, F.; Liu, Z.; Wang, W.; Shi, W.; Maginn, E. J. Absorption of CO₂ in the Ionic Liquid 1-n-Hexyl-3-Methylimidazolium Tris(Pentafluoroethyl)Trifluorophosphate ([Hmim][FEP]): A Molecular View by Computer Simulations. *J. Phys. Chem. B* **2009**, *113*, 7591–7598.
- (39) Dlubek, G.; Yu, Y.; Krause-Rehberg, R.; Beichel, W.; Bulut, S.; Pogodina, N.; Krossing, I.; Friedrich, C. Free Volume in Imidazolium Triflimide ([C₃MIM][NTf₂]) Ionic Liquid from Positron Lifetime: Amorphous, Crystalline, and Liquid States. *J. Chem. Phys.* **2010**, *133*, 124502.
- (40) Yu, Y.; Bejan, D.; Krause-Rehberg, R. Free Volume Investigation of Imidazolium Ionic Liquids from Positron Lifetime Spectroscopy. *Fluid Phase Equilib.* **2014**, *363*, 48–54.
- (41) Weber, C. C.; Brooks, N. J.; Castiglione, F.; Mauri, M.; Simonutti, R.; Mele, A.; Welton, T. On the Structural Origin of Free Volume in 1-Alkyl-3-Methylimidazolium Ionic Liquid Mixtures: A SAXS and ¹²⁹Xe NMR Study. *Phys. Chem. Chem. Phys.* **2019**, *21*, 5999–6010.
- (42) Margulis, C. J. Computational Study of Imidazolium-Based Ionic Solvents with Alkyl Substituents of Different Lengths. *Mol. Phys.* **2004**, *102*, 829–838.
- (43) Huang, X.; Margulis, C. J.; Li, Y.; Berne, B. J. Why Is the Partial Molar Volume of CO₂ So Small When Dissolved in a Room Temperature Ionic Liquid? Structure and Dynamics of CO₂ Dissolved in [Bmim⁺][PF₆⁻]. *J. Am. Chem. Soc.* **2005**, *127*, 17842–17851.
- (44) Almantariotis, D.; Gefflaut, T.; Pádua, A. A. H.; Coxam, J.-Y.; Costa Gomes, M. F. Effect of Fluorination and Size of the Alkyl Side-Chain on the Solubility of Carbon Dioxide in 1-Alkyl-3-Methylimidazolium Bis(Trifluoromethylsulfonyl)Amide Ionic Liquids. *J. Phys. Chem. B* **2010**, *114*, 3608–3617.
- (45) Forero-Martinez, N. C.; Cortes-Huerto, R.; Ballone, P. The Glass Transition and the Distribution of Voids in Room-Temperature Ionic Liquids: A Molecular Dynamics Study. *J. Chem. Phys.* **2012**, *136*, 204510.
- (46) Liu, H.; Zhang, Z.; Bara, J. E.; Turner, C. H. Electrostatic Potential within the Free Volume Space of Imidazole-Based Solvents: Insights into Gas Absorption Selectivity. *J. Phys. Chem. B* **2014**, *118*, 255–264.
- (47) Chrobok, A.; Swadźba, M.; Baj, S. Oxygen Solubility in Ionic Liquids Based on 1-Alkyl-3-Methylimidazolium Cations. *Pol. J. Chem.* **2007**, *81*, 337–344.
- (48) Vanhoutte, G.; Hojniak, S. D.; Bardé, F.; Binnemans, K.; Franssaer, J. Fluorine-Functionalized Ionic Liquids with High Oxygen Solubility. *RSC Adv.* **2018**, *8*, 4525–4530.
- (49) Hamza, M. H. A.; Serratrice, G.; Stebe, M. J.; Delpuech, J. J. Solute-Solvent Interactions in Perfluorocarbon Solutions of Oxygen. An NMR Study. *J. Am. Chem. Soc.* **1981**, *103*, 3733–3738.

(50) Serratrice, G.; Delpuech, J. J.; Diguët, R. Isothermal Compressibility of Fluorocarbons: Relationship with the Solubility of Gases. *Nouv. J. Chim.* **1982**, *6*, 489–493.

(51) Gomes, M. F. C.; Pádua, A. A. H. Interactions of Carbon Dioxide with Liquid Fluorocarbons. *J. Phys. Chem. B* **2003**, *107*, 14020–14024.

(52) Hayward, A. T. J. How to Measure the Isothermal Compressibility of Liquids Accurately. *J. Phys. D: Appl. Phys.* **1971**, *4*, 938–950.

(53) Clark, G. N. I.; Hura, G. L.; Teixeira, J.; Soper, A. K.; Head-Gordon, T. Small-Angle Scattering and the Structure of Ambient Liquid Water. *Proc. Natl. Acad. Sci. U.S.A.* **2010**, *107*, 14003–14007.

(54) Feigin, L. A.; Svergun, D. I. *Structure Analysis by Small-Angle X-Ray and Neutron Scattering*; Plenum Press, 1987.

(55) Pollice, R.; Chen, P. Origin of the Immiscibility of Alkanes and Perfluoroalkanes. *J. Am. Chem. Soc.* **2019**, *141*, 3489–3506.

(56) Xu, Y. CO₂ Absorption Behavior of Azole-Based Protic Ionic Liquids: Influence of the Alkalinity and Physicochemical Properties. *J. CO₂ Util.* **2017**, *19*, 1–8.

(57) Shimizu, K.; Almantariotis, D.; Gomes, M. F. C.; Pádua, A. A. H.; Canongia Lopes, J. N. Molecular Force Field for Ionic Liquids V: Hydroxyethylimidazolium, Dimethoxy-2-Methylimidazolium, and Fluoroalkylimidazolium Cations and Bis(Fluorosulfonyl)Amide, Perfluoroalkanesulfonylamide, and Fluoroalkylfluorophosphate Anions. *J. Phys. Chem. B* **2010**, *114*, 3592–3600.

(58) Almantariotis, D.; Gefflaut, T.; Pádua, A. A. H.; Coxam, J.-Y.; Costa Gomes, M. F. Effect of Fluorination and Size of the Alkyl Side-Chain on the Solubility of Carbon Dioxide in 1-Alkyl-3-Methylimidazolium Bis(Trifluoromethylsulfonyl)Amide Ionic Liquids. *J. Phys. Chem. B* **2010**, *114*, 3608–3617.